

## 11.2 DEEP CONVECTIVE CLOUD PHENOMENA IN THE UPPER TROPOSPHERE/LOWER STRATOSPHERE – A NEW DEVELOPMENT IN CLOUD SCIENCE

Pao K. Wang\*

University of Wisconsin-Madison, Madison, Wisconsin

### 1. INTRODUCTION

Recent discoveries of a few new phenomena atop many Midlatitude deep convective storms open up a new area for cloud research. The elucidation of these phenomena will not only help unraveling the physical processes involved in them, but also understanding the impacts of deep convective clouds on the large-scale and global atmospheric processes. This paper will give a summary of these findings and their implications to other fields.

### 2. STORM TOP PLUMES

This phenomenon was first discovered by meteorological satellite images that reveal the existence of chimney plume-like clouds atop the anvils of some severe thunderstorms (Setvak and Doswell, 1991; Levizzani and Setvak, 1996). Fig. 1 shows such an example. The plumes are generally about 3 km above the anvils. Since the anvils in some of these storms are already at the tropopause level, the plumes are thus most likely in the lower stratosphere. It was then unknown where the source of the moisture is for these plumes. The moisture could have been pre-existent in the stratosphere or could be transported from the storm below.

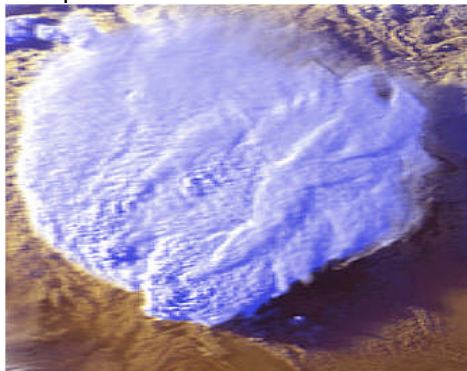


Fig.1. NOAA-12 AVHRR channels 1, 2 and 4 composite image of a thunderstorm on 11 September 1996 1724 UTC at Balearic Islands, Spain, showing the cirrus plume above the anvil. (Courtesy of M. Setvak)

To determine the plume moisture source, a 3-D nonhydrostatic quasi-compressible cloud model with explicit cloud microphysics, WISCDYMM (see Johnson et al., 1993, 1995; Lin et al., 2005), was used to perform simulations of a few severe thunderstorm cases typical of the US Midwest and Plains. The sounding used to initiate the simulation is the same as that in Johnson et al. (1993). The results of the simulated CCOPE supercell that occurred on 2 Aug 1981 in Montana will be used here for the discussion. The model results clearly demonstrate that the water vapor forming the plume comes from the storm below. Fig. 2 shows the simulated RHi (relative humidity with respect to ice) 30% contour surface. It demonstrated that the plume phenomenon is well-simulated and the size of the plume (as represented by the RHi iso-surface) is consistent with the observation. The general orientation is also consistent with the observed plumes, namely, along the central line of anvil and in the general direction of the upper level wind shear. The plume shown here appears to emanate from the overshooting top, which is also consistent with observation. Fig. 3 also shows the possibility of more than one plumes, which was also observed sometimes from satellite images (Levizzani and Setvak, 1996).

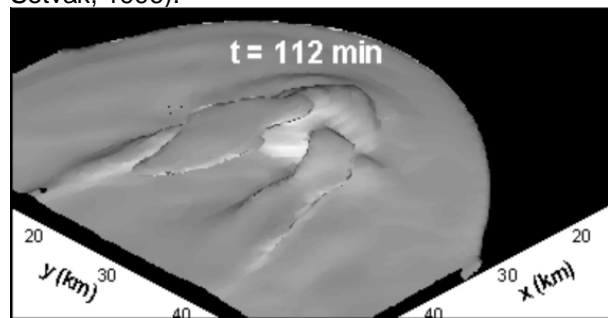


Fig.2. Simulated RHi = 30% surface of the CCOPE supercell storm at  $t = 112$  min, top view. The upper level winds are generally from upper right to the lower left (westerly) in the figure, i.e., along the orientation of the anvil top plume.

\*Corresponding author address: Pao K. Wang, Dept. of Atmospheric and Oceanic Sciences, University of Wisconsin-Madison, Madison, WI 53706. e-mail: [pao@windy.aos.wisc.edu](mailto:pao@windy.aos.wisc.edu).

Fig. 3 shows the central ( $y = 27$  km) east-west cross-sectional of the simulated storm. It is seen that the plume emanates from the overshooting

top and the plume layer centers at ~ 15 km, 3 km above the reported anvil layer of ~ 12 km of the

CCOPE storm, again consistent with the observation.

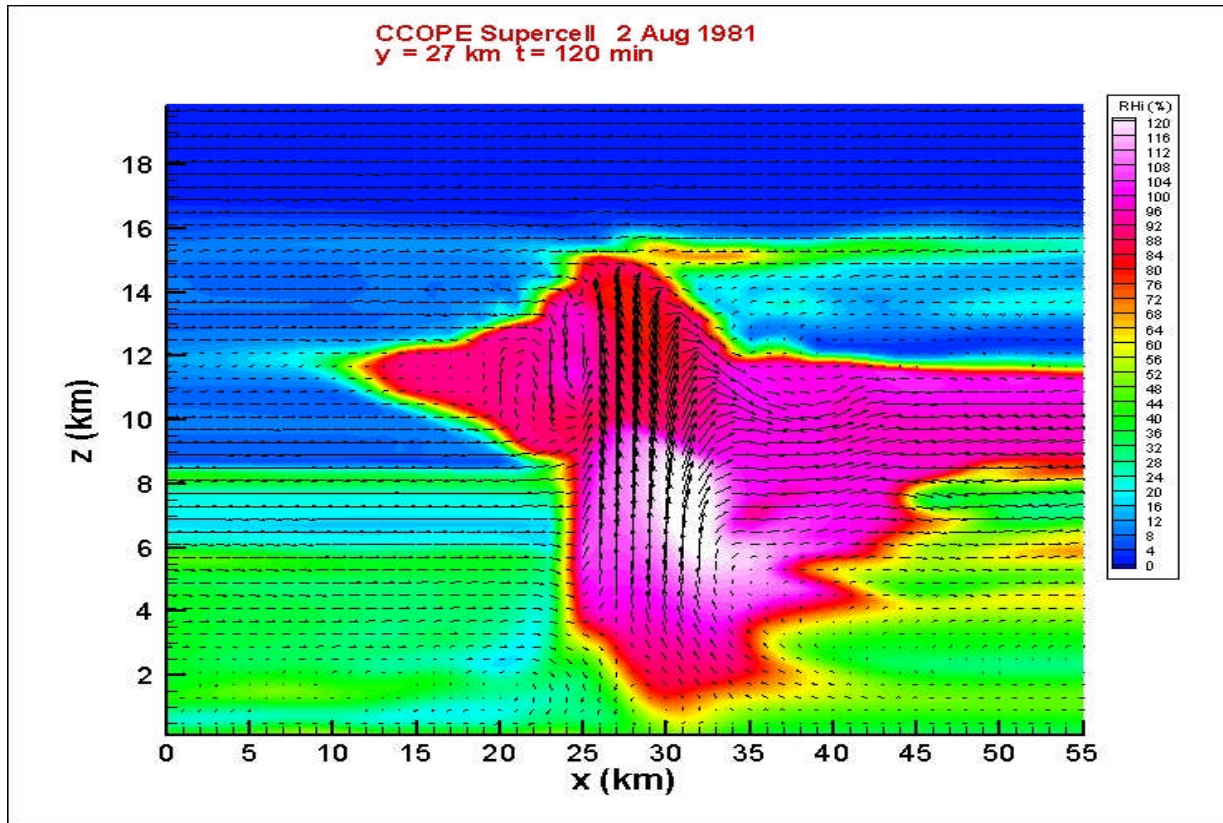


Fig. 3. Simulated CCOPE supercell central east-west cross-section RH field at  $t = 120$  min. Arrows are wind vectors projected on the  $x$ - $z$  plane.

Animations of the model results (to be shown during the conference) reveal that the plume water vapor source is from the storm cloud through the cloud top gravity wave breaking process. More details of this process have been given by Wang (2003, 2004, and 2005) and will also be briefly discussed in Sec. 3.

The confirmation that the plume source is the storm cloud has an important implication: it indicates that trace materials (e.g., water vapor, trace gases, aerosol particles) can be transported from the troposphere to the stratosphere by this gravity wave breaking mechanism. Some of these materials are strong greenhouse gases (for example, water vapor, methane, CFCs) that interact strongly with infrared (IR) radiation and hence may contribute to the global warming. The radiative interaction at the lower stratospheric level is known to be orders of magnitude higher than that in the lower troposphere, and hence the effect of this transport can be potentially important to the

global climate process. Wang (2003a) made an estimate of the amount of water vapor transported by this mechanism from the troposphere to the stratosphere and showed that it can be as high as 500 million tons per day. Adding the transport of other trace chemical species and the fact that  $H_2O$  is the precursor of ozone-depleting HOx and it becomes clear that the climatic and chemical impact to the stratosphere may be significant. This implies that deep convective clouds may play a role in the atmosphere far greater than the usually-conceived role of severe weather producer. At this moment, this mechanism and its effects have not been considered in any climate models.

### 3. FUJITA'S JUMPING CIRRUS

The second phenomenon is related to the jumping cirrus observed by Fujita in the 1980s who reported that "One of the most striking features seen repeatedly above the anvil top is the formation of cirrus cloud which jumps upward from behind the overshooting dome as it collapses

violently into the anvil cloud" (Fujita, 1982). In a later paper, Fujita (1989) classified 5 anvil top cirrus phenomena of which 3 are associated with obvious vertical motions. These three are: (1) *fountain cirrus* – cirrus which splashes up like a fountain, 1 to 2 min after an overshooting dome collapses into an anvil; (2) *flare cirrus* – cirrus that jumps 1 to 3 km above the anvil surface and moves upwind like a flare; (3) *geyser cirrus* – cirrus that bursts up 3 to 4 km above the anvil surface like a geyser. Fujita further indicated that the jumping cirrus will drift away from an overshooting area if the above-anvil winds are faster than the translational speed of the overshooting area. If not, the jumping cirrus moves back towards the overshooting area, which will be covered with a thin or thick veil of stratospheric cirrus. This implies that the cirrus would jump *upstream*. The cirrus clouds associated with the phenomena described here are generally known as the jumping cirrus.

No explanation of the possible mechanisms for the jumping cirrus were given in Fujita (1982, 1989) and there were doubts about whether or not cirrus can really jump upwind in a usually strongly sheared storm top environment. To investigate this problem, the same CCOPE supercell simulation results as described in the previous section were analyzed to see if one can observe this phenomenon from the simulated storm. The answer is affirmative.

Fig. 4 shows the RH<sub>i</sub> profile of the central east-west cross-section of the storm from t = 1320 to 2640 sec. Since the cloud top region is the focus here, these snapshots are windowed to 10-20 km vertically and 20-55 km horizontally, with the vertical scale stretched in these views. Note that the range of the vertical axis is from 10 to 20 km and that the general shear direction is from left to right (west to east).

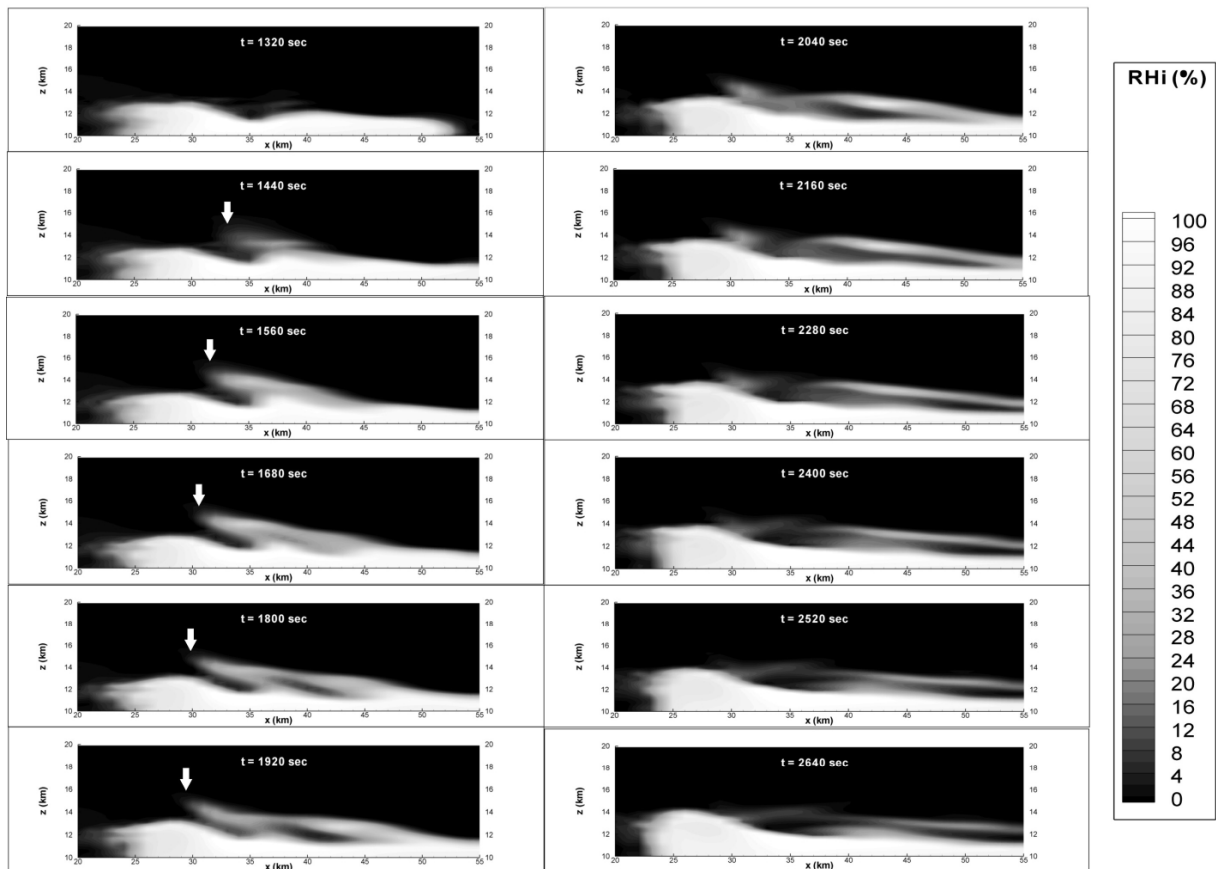


Fig. 4. Snapshots of the RH<sub>i</sub> profiles in the central east-west cross-section of the simulated CCOPE supercell storm from t = 1320 s to 2640 s.

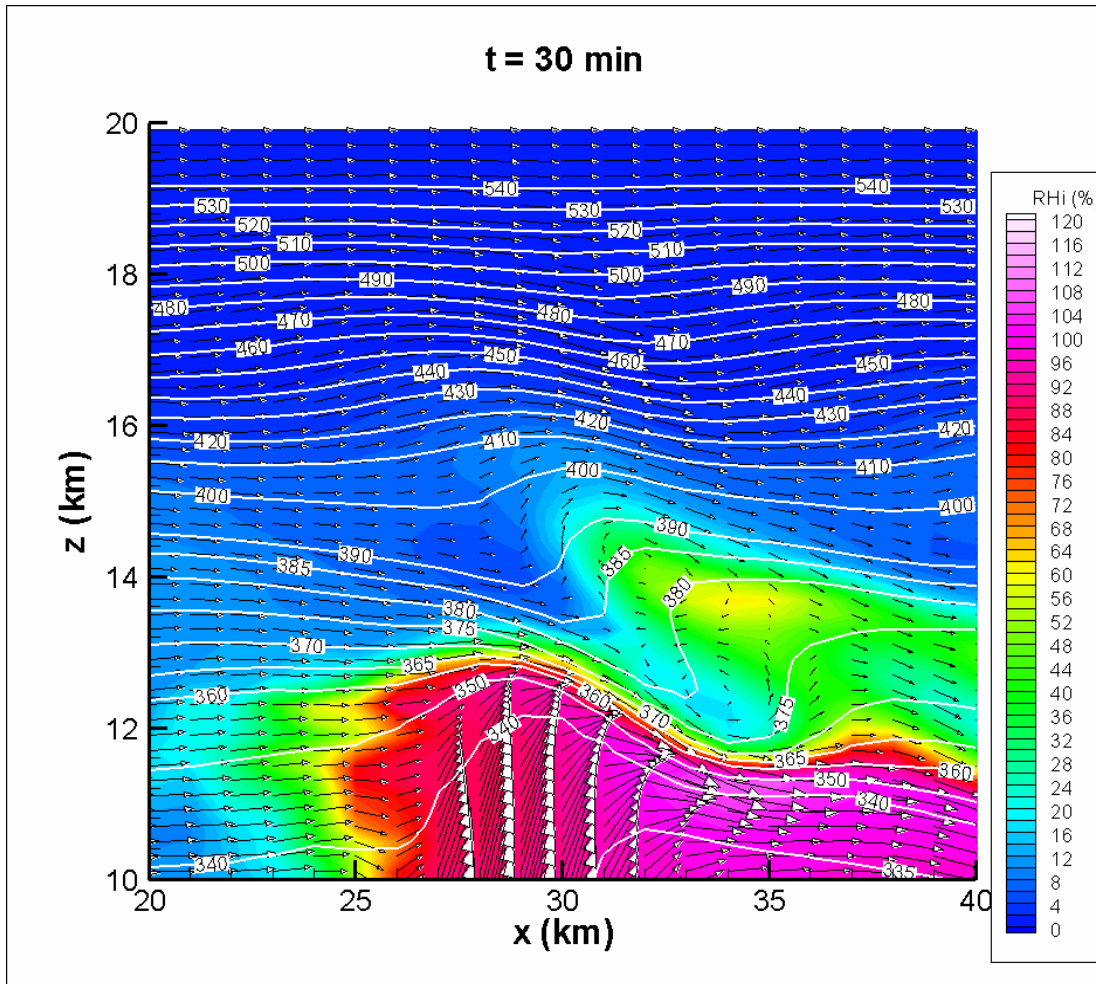


Fig. 5. The RH<sub>i</sub> and potential temperature fields in the central east-west cross-section of the simulated CCOPE supercell storm at  $t = 1800$  sec. The “wave-breaking” signature is most clearly seen in the  $\theta = 380$ K contour. Arrows represent wind vectors projected on the  $x$ - $z$  plane.

The front edge (visually defined by the brightness of the RH<sub>i</sub> profile) of the “jumping cirrus” was indicated by a white arrow. At  $t = 1320$  s, the storm top exhibits a two-wave pattern: one crest located at the main updraft region ( $x \sim 30$  km) and the other at  $x \sim 40$  km. At this stage the overshooting is not yet well developed and the highest point of the cloud is only slightly higher than the tropopause at 12.5 km (Johnson et al., 1993). However, the wavy nature of the storm top is already obvious. At  $t = 1440$  s, a cloudy patch starts to emanate from the bulge in the cloud top below. This humid patch is the precursor that eventually develops further into full-fledged jumping cirrus. The white arrow pointing at  $x \sim 34$  km indicates the approximate position of the left (west) edge of the patch. At the same time, the overshooting

top subsides, changing from a height of  $\sim 13$  km to  $\sim 12.5$  km, a drop of  $\sim 500$  m. This seems to correspond to what Fujita (1982) described as the “collapse of the overshooting dome”. While the overshooting top is subsiding, the wave crest located at  $x \sim 40$  km starts to bulge up and tilt upstream. At  $t = 1560$  s, a “jumping cirrus” in the form of a cirrus tongue has developed with its front edge located at  $x \sim 32$  km and reaching an altitude of  $\sim 15$  km. The cirrus tongue is already located higher than the overshooting top and is moving upstream. Note also that a third wave crest appears at  $x \sim 48$  km at this time. Thus the average “wavelength” of the waves on cloud top is approximately 9 km, although the distance between the first two upstream wave crests is only 6-7 km. The “tail” end of the jumping cirrus seems to originate from the detachment from the third wave crest.

As time goes on, the cirrus reaches further west and higher altitude as can be seen by the locations of the white arrows at the front edge. Since the altitudes of the jumping cirrus are both  $\sim 15$  km at  $t = 1560$  and  $1680$  s, the maximum altitude probably occurred somewhere in between these two times. This is best seen in Fig. 2 where the  $x$ ,  $z$  positions of the front edge of the cirrus are plotted as a function of time. The horizontal and vertical velocities are, of course, the corresponding slopes of these curves.

This upstream and upward motion corresponds to what Fujita described as the "cirrus cloud which jumps upward from behind the overshooting dome". This ascending sequence of the jumping cirrus lasts about 6 min within which the cirrus rises from  $z \sim 12$  km to  $\sim 15$  km. The average vertical speed of the jump is therefore about  $8 \text{ m s}^{-1}$ . This is a substantial vertical speed, indicating significant turbulence in that region, and is certainly justified to be described as "jumping". The development of the simulated cloud top up to this stage seems to verify Fujita's description of jumping cirrus.

What causes the cirrus to jump upward? This turns out to be again a gravity wave breaking phenomenon, like the anvil top plume formation described in Sec. 2. Fig. 5 shows the central east-west RHi cross-section at  $t = 30$  min overlaid with the potential temperature ( $\theta$ ) contours. The contour  $\theta = 380\text{K}$  indicates the breaking wave signature clearly and testifies that the jumping cirrus is caused by it. More details of the jumping cirrus mechanism can be found in Wang (2004).

Like the storm top plumes, the occurrence of jumping cirrus also signifies irreversible transport of materials from the troposphere to the stratosphere. Although the cirrus forms by the transport of  $\text{H}_2\text{O}$ , it is obvious that other trace species can be transported by the similar mechanism.

#### 4. PYRO-CUMULONIMBUS

The third is the formation of pyro-cumulonimbus (pyro-Cb) in areas affected by fire, which can occur in mid-latitude (such as

California) or even in high latitude locations (e.g., Alaska and Northern Canada).

With the help of heat energy released by forest or prairie fires and in a favorable synoptic environment, storms form that often penetrate the local tropopause that send ashes through the tropopause to reach lower stratosphere. Satellite images and data analysis show that sometimes ashes can reach very high into the stratosphere (e.g., Fromm et al., 2005a,b). Model simulations also indicate that strong convection caused by the addition of heat energy released by the fire can send ashes through the tropopause into the stratosphere (Wang, 2003; Winterrath et al., 2003). The pyro-Cb phenomenon in high latitude regions is of special importance because one usually do not associate these regions with strong convective activities. Yet the existence of the pyro-Cbs indicates that the high latitude sources cannot be ignored when considering global chemical transport. As Polar Regions are sensitive to climatic changes, it is important to investigate the implications of such cross-tropopause transport. Satellite images and model results will be shown during the conference.

#### 5. SUMMARY

All three phenomena described above are related to the deep convective cloud process near the tropopause. Traditional cloud physics studies are usually confined to lower to middle troposphere, mainly due to the relatively few observational platforms that can reach higher troposphere. Satellite techniques certainly are extremely useful but to interpret the data correctly we will need in-situ measurements and modeling.

The properties of clouds associated with these phenomena are poorly understood. Basic cloud microphysical works related to the very low temperature environment are only beginning (e.g., Bailey and Hallett, 2002, 2004; Wang, 2003, 2004, 2005; Mullendore et al., 2005). Potential research works are needed to understand these phenomena and their implications. This represents a new research area in cloud science that requires more studies.

**Acknowledgments.** This work is partially supported by the NSF Grant ATM-0244505 and University of Wisconsin-Madison WARF Grant 135-GA401.

## References

- Bailey, M., and J. Hallett, 2002: Nucleation effects on the habit of vapour grown ice crystals from  $-18^{\circ}\text{C}$  to  $-42^{\circ}\text{C}$ . *Quart. J. Roy. Meteor. Soc.*, **128**, 1461–1484.
- Bailey, M., and J. Hallett, 2004: Growth Rates and Habits of Ice Crystals between  $-20^{\circ}$  and  $-70^{\circ}\text{C}$ . *J. Atmos. Sci.*, **61**, 514–544.
- Fromm M., R. Bevilacqua, R. Servranckx, J. Rosen, J. P. Thayer, J. Herman, D. Larko, 2005a: Pyro-cumulonimbus injection of smoke to the stratosphere: Observations and impact of a super blowup in northwestern Canada on 3–4 August 1998. *J. Geophys. Res.*, **110**, D08205, doi:10.1029/2004JD005350.
- Fromm M., R. Bevilacqua, R. Servranckx, J. Rosen, J. P. Thayer, J. Herman, D. Larko 2005b: Correction to “Pyro-cumulonimbus injection of smoke to the stratosphere: Observations and impact of a super blowup in northwestern Canada on 3–4 August 1998”, *J. Geophys. Res.*, **110**, D12202, doi:10.1029/2005JD006171.
- Fujita, T. T., 1982: Principle of stereographic height computations and their application to stratospheric cirrus over severe thunderstorm. *Journal of Meteorological Society of Japan*, **60**, 355–368.
- Fujita, T. T., 1989: The Teton-Yellowstone tornado of 21 July 1987. *Mon. Wea. Rev.*, **117**, 1913–1940.
- Johnson, D. E., P. K. Wang, and J. M. Straka, 1993: Numerical simulation of the 2 August 1981 CCOPE supercell storm with and without ice microphysics. *J. Appl. Meteor.*, **32**, 745–759.
- Johnson, D. E., and P. K. Wang, and J. M. Straka, 1995: A study of microphysical processes in the 2 August 1981 CCOPE supercell storm. *Atmos. Res.* **33**, 93–123.
- Levizzani, V., and M. Setvak, 1996: Multispectral, high resolution satellite observations of plumes on top of convective storms, *J. Atmos. Sci.*, **53**, 361–369.
- Lin, Hsin-mu, Pao K. Wang, and Robert E. Schlesinger, 2005: Three-Dimensional Nonhydrostatic Simulations of Summer Thunderstorms in the Humid Subtropics versus High Plains. *Atmo. Res.* **78**, 103–145.
- Mullendore G. L., D. R. Durran, J. R. Holton, 2005: Cross-tropopause tracer transport in midlatitude convection, *J. Geophys. Res.*, **110**, D06113, doi:10.1029/2004JD005059.
- Setvak, M., and C. A. Doswell III, 1991: The AVHRR channel 3 cloud top reflectivity of convective storms, *Mon. Weather Rev.*, **119**, 841–847.
- Wang, P. K., 2003a: Moisture Plumes above Thunderstorm Anvils and Their Contributions to Cross Tropopause Transport of Water Vapor in Midlatitudes. *J. Geophys. Res.*, **108(D6)**, 4194, doi:10.1029/2003JD002581.
- Wang, P. K., 2003b : The Physical Mechanism of Injecting Biomass Burning Materials into the Stratosphere During Fire-induced Thunderstorms, *AGU Fall Meeting*, San Francisco, 2003.
- Wang, Pao K. 2004: A cloud model interpretation of jumping cirrus above storm top. *Geophys. Res. Lett.*, **31**, L18106, doi:10.1029/2004GL020787.
- Wang, Pao K. 2005: The Thermodynamic Structure atop a Penetrating Convective Thunderstorm. (in press (in press in *Atmospheric Research*))
- Winterrath, Tanja, Juerg Trentmann, Christiane Textor, Daniel Rosenfeld, Mike Fromm, RenT Servranckx, Pao K. Wang, Peter V. Hobbs, Meinrat O. Andreae, 2003: Modeling of Fire-Induced Supercell Convection and Transport of Biomass Burning Aerosol Into the Stratosphere: The Chisholm Fire of 28 May, 2001. *AGU Fall Meeting*, San Francisco, 2003.